A label-free strategy for facile electrochemical analysis of dynamic glycan expression on living cells†

Lin Ding,[a] Wei Cheng,[b] Xiaojian Wang,[a] Yadong Xue,[a] Jianping Lei,[a] Yibing Yin[b] and Huangxian Ju*[ab]

Received (in Cambridge, UK) 2nd September 2009, Accepted 30th September 2009
First published as an Advance Article on the web 14th October 2009
DOI: 10.1039/b918008g

A novel, label-free strategy has been developed for facile electrochemical analysis of dynamic glycan expression on living cells, which uses carbon nanohorns to efficiently immobilize lectin for the construction of a recognition interface and enhancing accessibility of cell surface glycan motifs.

Glycans, a class of intricate, informative biomacromolecules, participate in a myriad of key biological events, including protein–protein interactions, immune recognition/response, cell–cell communication, and intercellular signaling.[1] Abnormal alteration in cell surface glycan expression is associated with a variety of diseases, especially cancers.[2] Therefore, dynamic monitoring of carbohydrate motifs on cell surfaces has been recognized as a critical step toward deciphering the carbohydrate codes of a cell.[3]

Current efforts for decoding cell surface glycosylation have focused on mass spectrometric methods.[4] Although this technique can provide molecular details, it is time-consuming, and not amenable to living cell interrogation due to its destructive nature. The use of lectin–carbohydrate recognition specificities[5] provides an alternative non-destructive way for the analysis of glycans on living cells.[6–9] The developed methods utilize planar array[6,7] and probe-tagging[8,9] formats. They generally use fluorescent probes, nanoparticles or enzymes to label cells[6] or lectins.[8,9] However, the labeling of cells disturbs the cellular nature, and complexity and laboriousness are typically increased for a tagging protocol. Therefore it would be beneficial to develop label-free approaches to scrutinize glycan expression on living cells.

One label-free optical microscopy method for observing cell surface carbohydrate motifs has been reported.[7] But this method suffers from low sensitivity. Herein a novel label-free strategy for facile and specific electrochemical analysis of cell surface glycan expression was developed by combining rapid and sensitive electrochemical impedance spectroscopic (EIS) measurement with nanotechnology and using lectins as recognition units (Scheme 1). An effective three-dimensional recognition interface toward cell surface glycan motifs was constructed on a glassy carbon electrode (GCE) through stable immobilization of lectins on uniquely sphere-structured single-walled carbon nanohorns (SWNHs). Using unprocessed mammalian living tumor cells as a model, the glycan expression on cell surfaces was monitored through evaluation of the cell-capturing ability of the recognition interface.

The superstructured spherical SWNHs are typically composed of tubes of about 2–5 nm in diameter and 30–50 nm in length. The covalent attachment of lectins to oxygen-containing functional sites on SWNHs *via* 1-ethyl-3-(3-dimethylaminopropyl)carbodiimide as a coupling agent was verified through the infrared spectra and size expansion of the nanomaterials (Fig. S1 and S2 in ESI†).[10] The cell binding capacity of lectin-coupled SWNHs was 6 and 1.8 times that of single- and multi-walled CNTs, respectively (Fig. S3 in ESI†), showing the advantage of using SWNHs for cell capture and the retained recognition activity of lectins toward carbohydrate epitopes.

The binding extent of cells to lectin-immobilized electrodes was evaluated by monitoring the change of electron-transfer resistance (R_{et}) of $[Fe(CN)_6]^{3-/4-}$ as redox probes at a GCE (Fig. 1a).[11] The bare GCE showed a low resistance (curve A in Fig. 1a), and the successive assembly of the SWNH layer on the electrode surface significantly facilitated the interfacial electron transfer (curve B in Fig. 1a). After lectin coupling and subsequent BSA blocking, the electron transfer resistance increased using concanavalin A (Con A) as a model (curve C in Fig. 1a). Evidently, lectin acted as an inert electron- and mass-transfer blocking layer. The binding of cells to the Con A through specific recognition between cell surface glycan and the corresponding lectin immobilized on the electrode further hindered the access of the redox probes to the electrode,

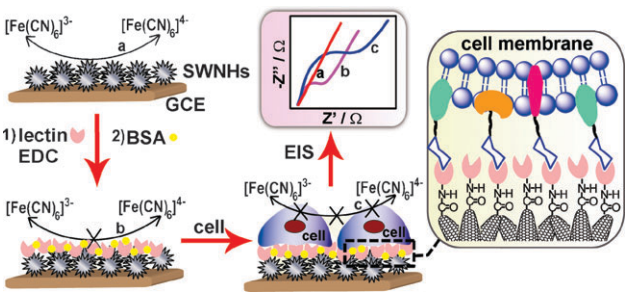

Scheme 1 Schematic representation of the electrochemical label-free strategy for the analysis of glycan expression on cell surfaces.

[a] *Key Laboratory of Analytical Chemistry for Life Science (Ministry of Education of China), Department of Chemistry, Nanjing University, Nanjing 210093, P. R. China. E-mail: hxju@nju.edu.cn; Fax: +86 25 83593593; Tel: +86 25 83593593*
[b] *Laboratory of Laboratory Medical Diagnostics (Ministry of Education of China), Department of Laboratory Medicine, Chongqing Medical University, Chongqing 400016, P. R. China*

† Electronic supplementary information (ESI) available: Experimental details, characterization of the conjugation, comparison of binding capability of lectin–carbon nanomaterials, and control experiment using flow cytometry. See DOI: 10.1039/b918008g

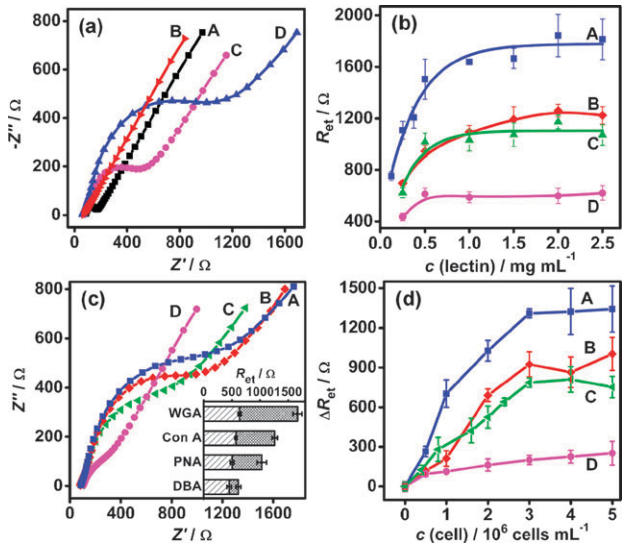

Fig. 1 (a) Electrochemical impedance spectra of (A) GCE, (B) SWNHs/GCE, (C) Con A-SWNHs/GCE and (D) K562 cells/Con A-SWNHs/GCE in 10 mM pH 7.4 phosphate buffered saline containing 0.1 M KCl, 5 mM $K_4Fe(CN)_6$ and 5 mM $K_3Fe(CN)_6$; (b) plots of R_{et} at (A) WGA, (B) Con A, (C) PNA, and (D) DBA-immobilized electrodes after incubation with 12 μL 2.0×10^6 cells mL^{-1} K562 cell suspension for 1 h *vs.* concentration of lectins; (c) impedance spectra of (A) WGA, (B) Con A, (C) PNA, and (D) DBA-covered electrodes after incubation with a K562 cell suspension at optimized lectin immobilization concentrations. Inset of (c): R_{et} values of lectin-covered electrodes after blocking with BSA (slash) and ΔR_{et} values for the increase of R_{et} upon cell binding (grid); and (d) plots of ΔR_{et} values at (A) WGA, (B) Con A, (C) PNA, and (D) DBA-immobilized electrodes *vs.* concentration of 12 μL K562 cell suspension for 1 h incubation.

leading to a high R_{et} value (curve D in Fig. 1a). The increase in magnitude of R_{et} (ΔR_{et}) correlated with the number of cells specifically bound to the electrode, which depended on the number of binding sites on cells captured by the lectin-covered electrode, and thus reflected the amount of target glycan expressed on the cell surfaces. The SWNHs increased both the surface area for cell binding and the electrical connectivity, thus improving the detection sensitivity.

In order to monitor the expression of different glycans on cell surfaces, four lectins with distinct binding specificities were coupled to SWNH-modified electrodes with the optimal lectin concentrations, respectively (Fig. 1b and Table S1 in ESI†). The ΔR_{et} values obtained at four lectin-immobilized electrodes upon incubation with the same cell concentration indicated a decreased cell binding ability in the order: wheat germ agglutinin (WGA) > concanavalin A (Con A) > peanut agglutinin (PNA) > *Dolichos biflorus* agglutinin (DBA) (Fig. 1c). These specific recognition-derived results reflected the expression extent of different glycans on cell surfaces, and suggested high expression of $(GlcNAc)_2$ and/or sialic acid, moderate expression of mannose, less Galβ1-3GalNAc and little GalNAc residues on the K562 cell surface. This difference provided fingerprinting glycan information on K562 cell surfaces, which was in accord with those obtained by flow cytometric analysis using fluorescein-lectin for recognition (Fig. S4 in ESI†) and previous reports,[6b,12] confirming the validity of the proposed method. This method needed 2.4×10^4 cells for whole detection, which was much less than the 3×10^5 and 9.5×10^5 cells required in lectin array-based methods,[6] demonstrating its sensitivity. The signal for cell binding could directly be observed during EIS detection, which was more quantitative and facile than microscopic observation.[7] Although the proposed method could not provide molecular details, it allowed insight to be gained into the most biologically-relevant surface-accessible glycan motifs.[6a]

At a fixed binding time, the impedance responses for different lectins were related to cell concentration used for binding (Fig. 1d). The signals obtained on WGA, Con A and PNA increased linearly with increasing cell concentration, and then tended to plateau at 3.0×10^6 cells mL^{-1} due to the limited binding sites and steric hindrance on lectin-SWNH modified electrode surfaces. The slope of plot of ΔR_{et} *vs.* cell concentration varied for different lectins (Fig. 1d), indicating different expression extents of these glycans. This result was identical with that obtained from Fig. 1c.

To validate the specificity of the interaction between cell surface glycan and lectin on an electrode, the immobilized lectin was firstly inhibited by corresponding monosaccharides (0.2 M) before cell incubation (Fig. 2).[6a,13] Mannose (Man) and *N*-acetylglucosamine (GlcNAc) notably inhibited the cell binding to Con A- and WGA-SWNH covered electrodes, respectively, while Man did not show any inhibition of the WGA-SWNH covered electrode, and the inhibition of GlcNAc of the Con A-SWNH covered electrode was less than 27%, suggesting negligible cross inhibition (Fig. 2b). The different inhibition abilities of Man and GlcNAc on corresponding electrodes were due to the variations in affinities of cells toward distinct lectins, caused by different extents of expression of carbohydrate epitopes.[6a]

Using 3′-azido-3′-deoxythymidine (AZT) as a model drug, which can inhibit nucleotide-sugar transport and significantly modify glycosylation on K562 cell surfaces,[12] this strategy was utilized to monitor the dynamic changes of cell surface glycans in response to drugs. The AZT-treated K562 cells displayed statistically greater ΔR_{et} on WGA-SWNH covered electrodes and lower ΔR_{et} on DBA-SWNH covered electrodes ($p < 0.05$), compared with control cells (Fig. 3), indicating greater exhibition of $(GlcNAc)_2$ and/or sialic acid and lower expression of terminal GalNAc on cell surfaces owing to the inhibition effect

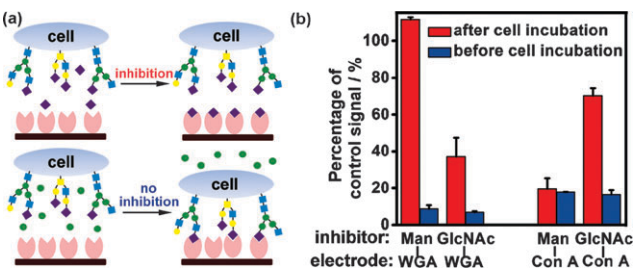

Fig. 2 Monosaccharide inhibition assay. (a) Scheme of the inhibition of monosaccharide against cell surface glycan for corresponding lectins. The inhibition was performed by preincubating the lectin-modified electrode in 200 mM Man or GlcNAc for 1 h before incubation with cells. (b) Percentage of control signal obtained on Man or GlcNAc-preincubated WGA (left) and Con A (right)-modified electrodes upon K562 cell incubation. Data were calculated by dividing the ΔR_{et} from monosaccharide-preincubated lectin-modified GCE by the ΔR_{et} from PBS-preincubated lectin-modified GCE.

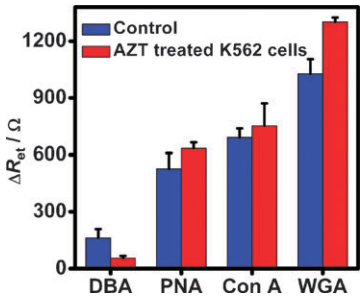

Fig. 3 ΔR_{et} values obtained on different lectin-immobilized electrodes after incubation with 12 μL cell suspension of AZT-treated K562 cells and control cells of 2.0×10^6 cells mL^{-1} for 1 h. The *p* values obtained by one-way ANOVA[6a] for the changes are 0.023, 0.10, 0.46 and 0.0059 (left to right).

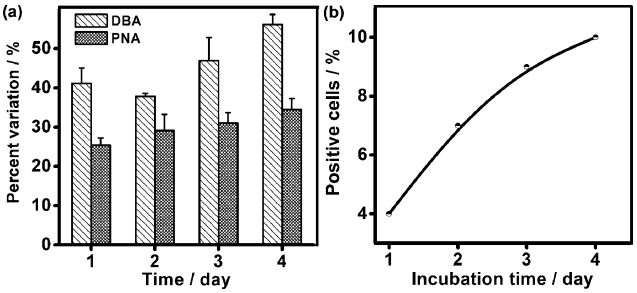

Fig. 4 Time-dependent effects of NaBu on erythroid differentiation of K562 cells. (a) The percent variation (Δ%) obtained on DBA (slash)- and PNA (grid)-immobilized electrodes was calculated as follows: $\Delta\% = [T/C - 1] \times 100\%$,[12] where *T* is the ΔR_{et} value obtained from incubation with NaBu-treated cells and *C* is that from untreated cells. Data shown are the mean values from three independent experiments, and error bars represent the S.D. of the mean. (b) Relationship between the percentage of staining-positive cell number and the incubation time.

of AZT on GalNAc glycan expression. The Con A did not give a statistically significant change ($p > 0.05$). Although the signal change of 20% for PNA was observed, which was greater than that of 15% from flow cytometry,[12] the change had less statistical significance. The signal change of 26% for WGA was less than the reported value of 44%, but the change trends were in good agreement.[9c,12] These results showed the effects of AZT on cell surface glycosylation, demonstrating that the proposed system could enable the elucidation of not only the presence or absence of a glycan epitope, but also subtle variations in the quantitative levels of exposed glycan residues.

This proposed strategy could also be employed for evaluation of the time-dependent glycosylation change during blood cell differentiation by treating K562 cells with sodium butyrate (NaBu, 1.0 mM) over 4 days.[6b,14] The differentiated cells revealed a progressive increase in the exhibition levels of Galβ1-3GalNAc and GalNAc residues as evidenced by the percent variation of ΔR_{et}[12] obtained on PNA and DBA-immobilized electrodes (Fig. 4a), whereas no substantial difference was observed for other lectins. These results suggested higher expression of O-glycan after the erythroid differentiation.[15] This trend was in agreement with the fluorescent microscopic glycan-profiling data for NaBu-treated K562 cells.[6b] The observed differentiation could be verified by a benzidine staining experiment (Fig. 4b). The increase in the number of benzidine staining-positive cells reflected the erythroid differentiation, in which O-glycosylation of glycophorin A in K562 cells increased.[14]

In summary, this work presents a label-free strategy for facile, rapid, and sensitive analysis of glycan expression on living cells. Using SWNHs for efficient immobilization of lectins, the constructed three-dimensional recognition interface can maintain the biological activity of the immobilized proteins, increase the cell binding capacity, and enhance the sensitivity for impedimetric analysis of the cell surface glycosignature. This method can be used for monitoring alteration of cell surface glycans in response to drugs and during biological events. This strategy obviates the use of complicated equipment, and could be further combined with an electrode array to achieve high-throughput label-free profiling of cell surface glycan expression. Future expansion of the knowledge base of carbohydrate–protein interactions will allow this strategy to gather even more detailed information about the glycome.

We thank Professor S. Iijima, leading the CNT project in the Japan Science and Technology Agency, for kindly providing single-walled carbon nanohorns. This work was funded by the National Natural Science Foundation of China (20821063, 90713015, 20535010, 20875044) and the National Basic Research Program of China (No. 2010CB732400).

Notes and references

1 R. Raman, S. Raguram, G. Venkataraman, J. C. Paulson and R. Sasisekharan, *Nat. Methods*, 2005, **2**, 817–824.
2 D. H. Dube and C. R. Bertozzi, *Nat. Rev. Drug Discovery*, 2005, **4**, 477–488.
3 K. T. Pilobello and L. K. Mahal, *Curr. Opin. Chem. Biol.*, 2007, **11**, 300–305.
4 X. Liu, D. J. McNally, H. Nothaft, C. M. Szymanski, J. -R. Brisson and J. Li, *Anal. Chem.*, 2006, **78**, 6081–6087.
5 H. Lis and N. Sharon, *Chem. Rev.*, 1998, **98**, 637–674.
6 (*a*) K. Hsu, K. T. Pilobello and L. K. Mahal, *Nat. Chem. Biol.*, 2006, **2**, 153–157; (*b*) H. Tateno, N. Uchiyama, A. Kuno, A. Togayachi, T. Sato, H. Narimatsu and J. Hirabayashi, *Glycobiology*, 2007, **17**, 1138–1146.
7 (*a*) T. Zheng, D. Peelen and L. M. Smith, *J. Am. Chem. Soc.*, 2005, **127**, 9982–9983; (*b*) S. Chen, T. Zheng, M. R. Shortreed, C. Alexander and L. M. Smith, *Anal. Chem.*, 2007, **79**, 5698–5702.
8 (*a*) Z. Zhelev, H. Ohba, R. Bakalova, R. Jose, S. Fukuoka, T. Nagase, M. Ishikawa and Y. Baba, *Chem. Commun.*, 2005, 1980–1982; (*b*) E. Nakata, Y. Koshi, E. Koga, Y. Katayama and I. Hamachi, *J. Am. Chem. Soc.*, 2005, **127**, 13253–13261.
9 (*a*) L. Ding, W. Cheng, X. Wang, S. Ding and H. Ju, *J. Am. Chem. Soc.*, 2008, **130**, 7224–7225; (*b*) W. Cheng, L. Ding, J. Lei, S. Ding and H. Ju, *Anal. Chem.*, 2008, **80**, 3867–3872; (*c*) W. Cheng, L. Ding, S. J. Ding, Y. B. Yin and H. X. Ju, *Angew. Chem., Int. Ed.*, 2009, **48**, 6465–6468.
10 (*a*) M. Zhang, M. Yudasaka, K. Ajima, J. Miyawaki and S. Iijima, *ACS Nano*, 2007, **1**, 265–272; (*b*) W. Tu, J. Lei, L. Ding and H. Ju, *Chem. Commun.*, 2009, 4227–4229.
11 L. J. Yang, Y. B. Li and G. F. Erf, *Anal. Chem.*, 2004, **76**, 1107–1113.
12 A. R. Lizzi, A. M. D'Alessandro, A. Bozzi, B. Cinque, A. Oratore and G. D'Andrea, *Mol. Cell. Biochem.*, 2007, **300**, 29–37.
13 K. T. Pilobello, D. E. Slawek and L. K. Mahal, *Proc. Natl. Acad. Sci. U. S. A.*, 2007, **104**, 11534–11539.
14 C. G. Gahmberg, M. Ekblom and L. C. Andersson, *Proc. Natl. Acad. Sci. U. S. A.*, 1984, **81**, 6752–6756.
15 H. Sasaki, B. Bothner, A. Dell and M. Fukuda, *J. Biol. Chem.*, 1987, **262**, 12059–12076.

Electronic Supplementary Information (ESI) for Chemical Communications

A label-free strategy for facile electrochemical analysis of dynamic glycan expression on living cells

Lin Ding, Wei Cheng, Xiaojian Wang, Yadong Xue, Jianping Lei, Yibing Yin and Huangxian Ju*

Key Laboratory of Analytical Chemistry for Life Science (Education Ministry of China), Department of Chemistry, Nanjing University, Nanjing 210093, P.R. China; and Key Laboratory of Laboratory Medical Diagnostics (Ministry of Education of China), Department of Laboratory Medicine, Chongqing Medical University, Chongqing 400016, P.R. China

Experimental

Materials. Concanavalin A (Con A), wheat germ agglutinin (WGA), Dolichos bifows agglutinin (DBA), bovine serum albumin (BSA), 1-ethyl-3-(3-dimethylaminopropyl) carbodiimide (EDC) and 3′-Azido-3′-deoxythymidine (AZT) were purchased from Sigma-Aldrich Inc. (USA). Peanut agglutinin (PNA) was purchased from Medicago Inc. (Sweden). Fluorescein-labeled WGA (molar ratio of fluorescein/protein, F/P = 4.5), Con A (F/P = 5.7), PNA (F/P = 5.1), DBA (F/P = 2.2) were from Vector laboratories (Burlingame, USA). Mannose (Man) and *N*-acetylglucosamine (GlcNAc) with analytical grade were from Sinopharm Chemical Reagent Co., Ltd (China). Single-walled carbon nanohorns (SWNHs) were kindly provided by Prof. S. Iijima (Japan Science and Technology Agency). Single-walled carbon nanotubes (SWNTs, ≤ 2 nm in diameter; 5-15 μm in length) and multi-walled carbon nanotubes (MWNTs, 20-40 nm in diameter; 5-15 μm in length) were from Shenzhen Nanotech Co. (China). Phosphate buffer saline (PBS, pH 7.4) contained 136.7 mM NaCl, 2.7 mM KCl, 8.72 mM Na_2HPO_4, and 1.41 mM KH_2PO_4. All

other reagents were of analytical grade. All aqueous solutions were prepared using ultra-pure water (≥ 18 MΩ, Milli-Q, Millipore). SWNHs were dispersed in 30% HNO_3 and then refluxed for 24 h at 140 °C to obtain carboxylic group-functionalized SWNHs. The resulting suspension was centrifuged, and the sediment was washed with deionized water until the pH reached 6.0. Then, the oxidized SWNHs were dispersed in deionized water to a concentration of 0.5 mg mL^{-1}. Oxidized SWNTs and MWNTs were produced by the same procedure.

Cell culture and cell treatment. K562 cell line was kindly provided by the Affiliated Zhongda Hospital, Southeast University, Nanjing, China. K562 cells were cultured in a flask in RPMI 1640 medium (GIBCO) supplemented with 10% fetal calf serum (FCS, Sigma), penicillin (100 μg mL^{-1}) and streptomycin (100 μg mL^{-1}) at 37 °C in a humidified atmosphere containing 5% CO_2. The cells in the exponential growth phase were collected and separated from the medium by centrifugation at 1000 rpm for 3 min, and then washed three times with a sterile pH 7.4 PBS. The sediment was re-suspended in the PBS to obtain a homogeneous cell suspension. Cell number was determined using a Petroff-Hausser cell counter (USA). AZT-treated K562 cells were obtained by incubating the cells in culture medium in the presence of 20 μM AZT for 3 h. The K562 cells were differentiated to erythroid lineages for 4 days by addition of 1 mM sodium butyrate (NaBu) in culture medium.

Electrode preparation. The glassy carbon electrode (GCE) was firstly polished with 1.0, 0.3, and 0.05 μm α-Al_2O_3 powder (Beuhler) successively. After sonication in water, the electrode was rinsed with deionized water and allowed to dry at room temperature. SWNH solution (6 μL, 0.5 mg mL^{-1}) was dropped on the pretreated GCE and dried in a desiccator to obtain SWNHs-coated GCE, which was then immersed in 8 μL PBS solution containing 2.5 mM EDC and optimal concentration of lectin for 3 h to yield lectin-immobilized electrode. Following a rinse with 0.01 M pH 7.4 PBS, the modified electrode was soaked in 50 mM pH 7.4 Tris-HCl buffer containing 1% BSA and 0.1 M NaCl for 30 min to block the surface. 12 μL of 2.0×10^6 cells mL^{-1} K562 cell suspension was dropped on the lectin-immobilized electrode and incubated at 25 °C for 1 h. After careful rinsing with 0.01 M pH 7.4 PBS to remove

noncaptured cells, the obtained electrode was ready for impedance measurement. For Con A-immobilized electrode, 1 mM Ca^{2+} and Mn^{2+} should be added to the recognition solution.

M**onosaccharide inhibition assay**. The lectin-immobilized electrode was preincubated with 12 μL 200 mM monosaccharide (Man or GlcNAc) dissolved in PBS for 1 h at 25 °C.[1] Then 2 μL of K562 cell suspension at 1.4×10^7 cells mL^{-1} was added to the monosaccharide solution on electrode surface and incubated for 1 h at 25 °C. After careful rinsing with PBS to remove the noncaptured cells and sugar, the electrode was used for impedance assay. Data shown are the percentage of control signals (the ΔR_{et} from monosaccharide-preincubated lectin modified GCE divided by the ΔR_{et} from PBS-preincubated lectin modified GCE).

Optimization of lectin modification concentration. Lectins were dissolved in 0.01 M pH 7.4 PBS containing 2.5 mg mL^{-1} EDC at different concentrations (from 0.25 mg mL^{-1} to 2.5 mg mL^{-1}), and then 8 μL of the mixture was deposited on SWNH-coated GCE. After coupling, BSA blocking, and cell capturing steps, the obtained cell-captured electrodes were subjected to impedance measurements.

Examination on the effect of cell concentration. To demonstrate the cell concentration-dependent signal change, the lectin-immobilized electrodes were incubated with 12 μL of K562 cell suspension at certain concentrations from 5×10^5 to 5×10^6 cells mL^{-1} for 1 h at 25 °C. After careful rinsing with 0.01 M pH 7.4 PBS, the electrodes were subjected to impedance measurements.

Comparison of the cell binding capacity. 0.5 mg mL^{-1} oxidized SWNHs, SWNTs and MWNTs were dropped on glass slides, respectively, and dried in a desiccator. The subsequent WGA immobilization, BSA blocking and cell incubation steps were the same as described above. The obtained slides were subjected to optical microscopic observation.

Flow cytometry analysis of glycan expression pattern on K562 cell surface. K562 cells were collected by centrifugation at 1000 rpm for 6 min at room temperature. After the cells were washed with cold PBS, they were resuspended in PBS at a concentration of 1×10^7 cells mL^{-1}. 50 μL cell suspension was then added to the mixture of 445 μL PBS and 5 μL 2 mg mL^{-1} fluorescein-labeled lectin. For fluorescein-

labeled Con A, 1 mM Ca^{2+} and Mn^{2+} were added to the recognition solution. After incubation for 30 min, the cells were collected by centrifugation at 1000 rpm for 6 min, washed with PBS, resuspended in 500 μL PBS, and assayed by flow cytometry. Unlabeled K562 cells were used as the negative control for estimation of autofluorescence, and relative cell-associated fluorescent intensity was obtained by subtraction of autofluorescence. For comparison purpose, the obtained relative cell-associated fluorescent intensity was standardized with the molar ratio of fluorescein/protein.

Benzidine staining experiment. 50 μL cell suspension at 1×10^6 cells mL^{-1} was mixed with 10 mL benzidine reagent containing 0.6% H_2O_2, 0.5 M acetic acid and 0.2% benzidine dihydrochloride. The percentage of benzidine staining-positive cells (blue cells) was determined by light microscopic examination of 100 cells per sample.[2]

Apparatus and characterization. The morphologies of SWNHs coated on GCE (3 mm diameter) and lectin-functionalized SWNHs/GCE were observed under a Hitachi S-4800 scanning electron microscopy (SEM, Japan) and a JEOL JEM-2100 transmission electron microscopy (TEM, Japan). Optical microscopic images were obtained by Nikon TE2000-U inverted fluorescence microscope (Japan). Infrared spectra were recorded on a Nicolet 400 Fourier transform infrared spectrometer (Madison, WI). Flow cytometry was carried out on a FACS Calibur flow cytometer (Becton Dickinson, USA). Electrochemical impedance spectroscopic measurements were performed on a PGSTAT30/FRA2 system (Autolab, Netherlands) in 10 mM pH 7.4 PBS containing 5 mM $K_4Fe(CN)_6$, 5 mM $K_3Fe(CN)_6$ and 0.1 M KCl using a conventional three-electrode system with modified GCE as working, platinum wire as auxiliary, and saturated calomel electrode as reference electrodes. Typical impedance spectrum includes a semicircle portion and a linear line portion, which correspond to the electron transfer process and diffusion process, respectively. The diameter of the semicircle represents the electron-transfer resistance at the electrode surface. The impedance spectra were recorded within the frequency range of 5×10^{-2} – 10^5 Hz. The amplitude of the applied sine wave potential was 5 mV. All the experiments were performed at 25 °C. All R_{et} value was obtained from three independent experiments, and error bars represent the S.D. of the mean.

Infrared characterization of coupling of lectin to SWNHs[3]

After Con A coupling, two new absorption bands corresponding to amide band I (C=O stretching) and II (N-H bending) appeared at 1640 and 1525 cm^{-1}, respectively, and the peaks at 1723 and 1581 cm^{-1} attenuated.

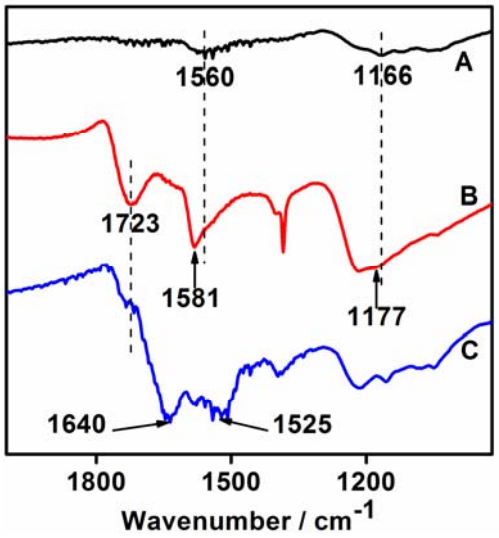

Fig. S1. Infrared spectra of (A) SWNHs, (B) oxidized SWNHs and (C) Con A-SWNHs conjugates.

SEM and TEM characterization of lectin coupling to SWNHs.

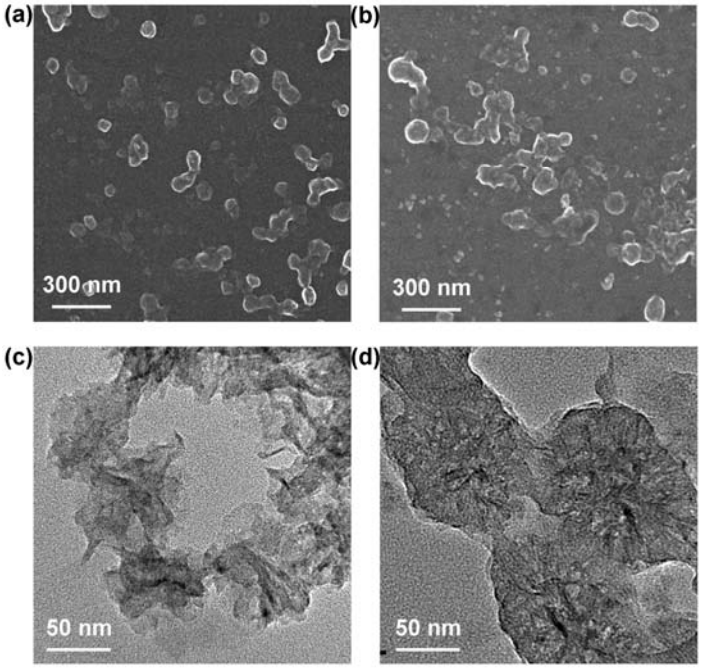

Fig. S2 SEM images of (a) SWNHs/GCE and (b) Con A-SWNHs/GCE, and TEM images of (c) SWNHs and (d) Con A-SWNHs conjugates.

Comparison of cell capture capacity of lectin-functionalized carbon nanomaterials

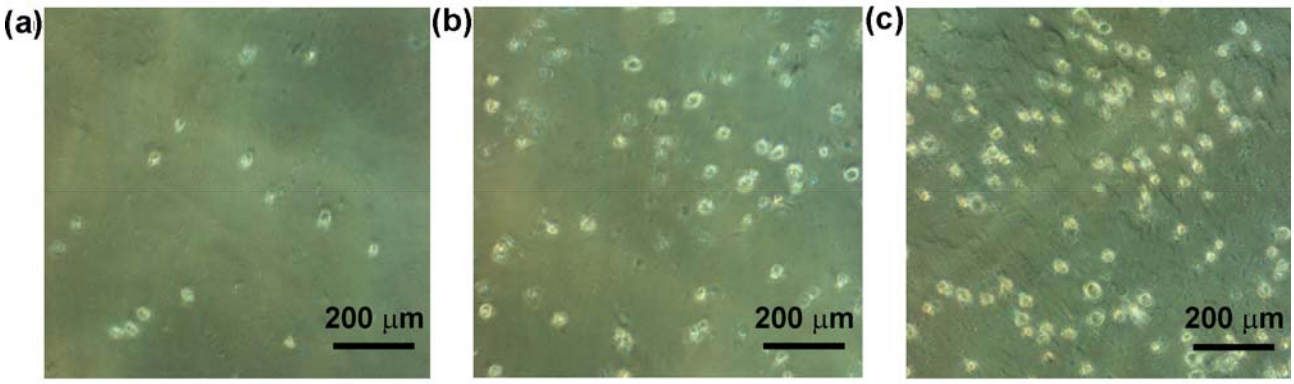

Fig. S3 Optical microscopic images of K562 cells captured on WGA-functionalized (a) single-walled carbon nanotubes, (b) multi-walled carbon nanotubes and (c) SWNHs on glass slides. The nanomaterial interface was fabricated by the same procedure as described in the Experimental section.

Table S1 Carbohydrate-binding specificities of the lectins used in this work[4]

Lectins	Origin	Binding specificity[a]	Optimized concentration for immobilization (mg mL^{-1})
Con A	*Canavalia ensiformis*	terminal α-Man, Manα3(Manα6)Man	2.0
DBA	*Dolichos biflorus*	GalNAcα-Ser/Thr (Tn), GalNAcα1-3GalNAc	0.5
PNA	*Arachis hypogaea*	Galβ1-3GalNAcα-Ser/Thr, Galβ1-3GalNAcβ1-4Galβ	1.0
WGA	*Triticum unlgari*	$(GlcNAc)_n$, multivalent Sia	1.5

[a] Man, mannose; GalNAc, *N*-acetylgalactosamine; Gal, galactose; Sia, sialic acid; GlcNAc, *N*-acetylglucosamine; Ser, serine; Thr, threonine.

Flow cytometric analysis of the glycan expression pattern on K562 cell surface

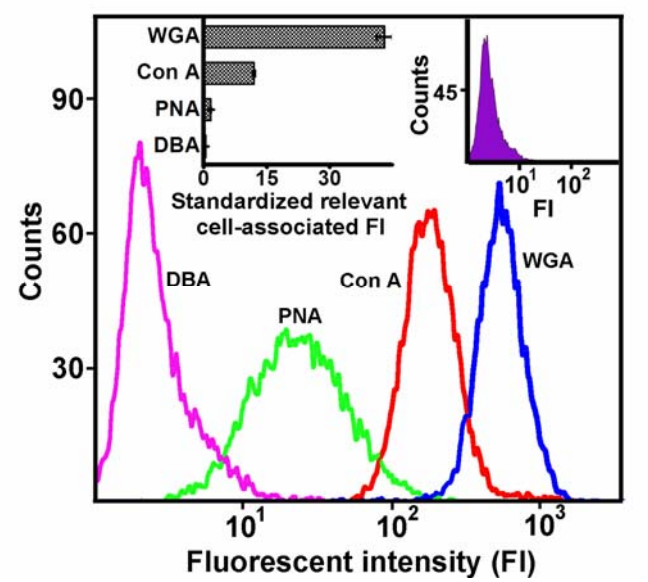

Fig. S4 Flow cytometric analysis of lectin-binding sites on K562 cells with fluorescein-labeled DBA, PNA, Con A, and WGA at room temperature. Inset: standardized relative cell-associated fluorescent intensity of K562 cells after incubation with fluorescein-labeled lectins (*left*), and autofluorescence of unlabeled K562 cells (*right*).

References

1 K. T. Pilobello, D. E. Slawek and L. K. Mahal, *Proc. Nat. Acad. Sci. USA*, 2007, **104**, 11534-11539.

2 N. Belhacène, L. Maulon, S. Guérin, J. E. Ricci, B. Mari, Y. Colin, J. P. Cartron and P. Auberger, *FASEB J.*, 1998, **12**, 531-539.

3 M. Zhang, M. Yudasaka, K. Ajima, J. Miyawaki and S. Iijima, *ACS Nano*, 2007, **1**, 265-272.

4 K. A. Wearne, H. C. Winter, K. O'Shea and I. J. Goldstein, *Glycobiology*, 2006, **16**, 981-990.